Proceedings of the Research Institute of Atmospherics,
Nagoya University, vol. 36 (1989) -Research Report-

THE EFFECTS OF DIPOLE TILT ON MAGNETOTAIL STRUCTURE AND DYNAMICS

Tatsuki Ogino, Raymond J. Walker[1], and Maha Ashour-Abdalla[1,2]

[1]Institute of Geophysics and Planetary Physics
University of California
Los Angeles, California 90024-1567, U. S. A.
[2]Department of Physics
University of California
Los Angeles, California 90024-1567, U. S. A.

Abstract

A three-dimensional time-dependent global magnetohydrodynamic (MHD) model of the interaction between the solar wind and the earth's magnetosphere has been used to study the effects of dipole tilt on the structure and dynamics of the magnetotail. The location of the tail neutral sheet shifts in the north-south direction following changes in the dipole tilt. When the northern edge of the geomagnetic dipole is tilted toward the sun, namely for positive tilt, it is above the geocentric solar magnetosphere (GSM) equator, while for negative tilt it is below. The neutral sheet forms an arc across the tail in the y-z plane for non-zero tilt. For positive tilt, the neutral sheet rises above the GSM equatorial plane near the noon-midnight meridian and returns to the equator near the magnetopause. Such cross-sectional behaviour of the neutral sheet is similar to that deduced from observations by Fairfield. The position and shape of the neutral sheet result from the requirement that the earthward magnetic flux equals the tailward flux and can be well explained by a simple analytical model.

1. Introduction

Dipole tilt of the geomagnetic field in the sun-earth meridian as well as the existence of non-zero x-component of the interplanetary magnetic field (IMF) can

fundamentally create a north-south asymmetry in the earth's magnetospheric structure. The magnetic equator directly responds to the dipole tilt and is formed on the plane perpendicular to the dipole axis near the earth. It has been demonstrated from observations that the magnetic neutral sheet extends straight toward the anti-sunward direction in the distant tail near the midnight meridian as a result of the interaction with the solar wind, though the magnetic equator (or neutral sheet) keeps an inclined angle within a distance (about $10Re$) less than the radius of the magnetopause, where Re stands for the radius of earth [*Bame et al.*, 1967; *Bowling*, 1974; *Bowling and Russell*, 1976; *Fairfield and Ness*, 1970; *Murayama*, 1966; *Rosenbauer et al.*, 1975; *Russell and Brody*, 1967; *Speiser and Ness*, 1967]. Thus, the neutral sheet is raised up along the magnetic equator in the near tail and becomes parallel to the solar wind flow direction in the distant tail when the northern part of the geomagnetic dipole is tilted toward the sun (positive tilt). The hinging distance is about a half the radius of magnetopause (about $x = -10R_e$) in the tail and is also associated with the transition region from the dipole-like magnetic field to the elongated tail-like field.

The raised neutral sheet above the gyrocentric solar magnetospheric (GSM) equatorial plane simultaneously forms an arched surface around the local midnight in the tail cross section, however it is depressed below the plane near the magnetopause flanks. The empirical neutral sheet model in the tail cross section was demonstrated by Fairfield [1980] from spacecraft measurements of the tail field polarity and was again compared with the ISEE 2 plasma and magnetic field data in the nearer earth tail by Gosling et al. [1986]. The Fairfield empirical model could well explain the observational result when the proper three parameters to determine the shape of neutral sheet were adopted. The feature of the magnetic neutral sheet can be understood to be physically more preferable because the area of the tailward magnetic flux is closer to that of the earthward flux in the tail cross section. Moreover, the neutral sheet on flanks should be naturally depressed below the GSM equatorial plane due to the dynamical effect during northern hemisphere summer because it is formed by the convection of the depressed magnetic field lines from the dayside magnetosphere toward the tail flanks. Thus the Fairfield's empirical model is regarded as a reasonable neutral sheet model for a small tilt angle, however it still has three problems to be considered: the first is that there are three free parameters to adjust the shape of neutral sheet, the second is that the area below the neutral sheet differs slightly from the area above it, and the third is that the empirical formula is not applicable for a larger tilt angle. For example, the neutral sheet must be a ring when the dipole axis points to the sun. Of course, such an extreme condition is not realistic for the earth's magnetosphere, however a larger dipole tilt may occur for other planets like Uranus [*Siscoe*,1971; *Ness et al.*, 1986].

The configuration of the tail plasma sheet was theoretically calculated in connection with a three-dimensional magnetic field model of the earth's magnetosphere by Voigt [1981, 1984]. He used a separation method assuming a cylindrical magne-

totail boundary with a constant radius and found a plasma sheet structure which agrees qualitatively with Fairfield's empirical neutral sheet model. The magnetospheric structure as a function of dipole tilt was also studied by using a global magnetohydrodynamic (MHD) model by Wu [1984]. He showed that the calculated shape and positions of the magnetic neutral sheet are consistent with the Fairfield's empirical formula for a small tilt angle of $\theta = 30°$; however, they deviate somewhat from the formula for a larger tilt angle of $\theta = 75°$.

In the present paper, the effects of dipole tilt on the structure and dynamics of the earth's magnetotail have been studied from a theoretical analysis as well as 2- and 3-dimensional global MHD simulations of the interaction between the solar wind and the magnetosphere. The shape and positions of the magnetic neutral sheet will be presented for all the dipole tilt angles from the simulation, and their characteristic features will be discussed in comparison with a theoretical model and observational materials.

2. Simulation Model

The simulation model will be briefly reviewed because it is described in detail elsewhere [*Ogino*, 1986; *Ogino et al.*, 1985]. Our present purpose is to study the effects of dipole tilt in the sun-earth meridian on the magnetospheric structure from the 2- and 3-dimensional global MHD simulations. The dipole tilt should create a north-south hemispheric asymmetry in the earth's magnetospheric configuration. Therefore, we need to solve the MHD and Maxwell's equations for both the northern and southern hemispheres as an initial value problem by using the two-step Lax-Wendroff scheme. The normalized MHD equations are written as follows,

$$\frac{\partial \rho}{\partial t} = -\vec{\nabla} \cdot (\vec{v}\rho) + D\nabla^2 \rho \tag{1a}$$

$$\frac{\partial \vec{v}}{\partial t} = -(\vec{v} \cdot \vec{\nabla})\vec{v} - \frac{1}{\rho}\vec{\nabla} p + \frac{1}{\rho}\vec{J} \times \vec{B} + \frac{1}{\rho}\vec{\Phi} \tag{1b}$$

$$\frac{\partial p}{\partial t} = -(\vec{v} \cdot \vec{\nabla})p - \gamma p \vec{\nabla} \cdot \vec{v} + D_p \nabla^2 p \tag{1c}$$

$$\frac{\partial \vec{B}}{\partial t} = \vec{\nabla} \times (\vec{v} \times \vec{B}) + \eta \nabla^2 \vec{B} \tag{1d}$$

$$\vec{J} = \vec{\nabla} \times (\vec{B} - \vec{B}_d), \tag{1e}$$

where ρ is the plasma density, $\vec{v}$ the flow velocity, p the plasma pressure, $\vec{B}$ the magnetic field, $\vec{B}_d$ the dipole field, $\vec{J}$ the current density, $\vec{g}$ the gravity force, $\vec{\phi} \equiv \mu\nabla^2\vec{v}$ the viscosity, $\gamma = 5/3$ the ratio of the specific heats, $\eta = \eta_0(T/T_0)^{-3/2}$ the

resistivity and T/T_0 is the temperature normalized by its value in the ionosphere. The units for distance, velocity, and time are the earth's radius, $Re = 6.37 \times 10^6 m$, the Alfvén speed at one earth radius on the equator, $v_A = 6.80 \times 10^6 m/s$ and the Alfvén transit time, $t_A = R_e/v_A = 0.937s$. The numerical coefficients are $\eta_0 = 0.01$, $\mu/\rho_{sw} = D = D_p = 0.003$, where ρ_{sw} is the solar wind density. The values of μ, D and D_p were selected appropriately to be small in order not to have significant influence on the global structure and also in order to suppress MHD fluctuations with grid interval. The magnetic Reynold's number, which is the magnetic diffusion time divided by the Alfvén transit time, is $S = 100 - 1000$.

The solar magnetospheric coordinate system is used in the calculation. A uniform solar wind with $n_{sw} = 5/cm^{-3}$, $v_{sw} = 300\ km/s$ and $T_{sw} = 2 \times 10^{5o} K$ flows into a simulation box of dimensions, $x_0 \leq x \leq x_1$, $0 \leq y \leq y_0$ and $-z_0 \leq z \leq z_0$ at $x = x_1$, where typically $x_0 = -60R_e$, and $x_1 = y_0 = z_0 = 30R_e$. Free boundary conditions, where the derivatives of all physical quantities are zero, are used at $x = x_0$, $y = y_0$, and $z = \pm z_0$. A mirror boundary condition was used at $y = 0$, that is $\psi(-y, z) = \psi(y, z)$; for ρ, v_x, v_z, p, B_x and B_z, on the other hand, $\psi(-y, z) = -\psi(y, z)$ for v_y and B_y. Moreover, the simple ionospheric boundary condition imposed near the earth was determined by requiring a static equilibrium [*Ogino*, 1986]; in this way all the parameters are held constant for $\xi \equiv (x^2 + y^2 + z^2)^{1/2} < 3.5R_e$ and all perturbations are damped out by using a smoothing function near the ionosphere ($\xi \leq 5.5Re$). Therefore, the field aligned currents also disappear near the earth and do not close in the ionosphere. The MHD equations were solved on a $(N_x, N_y, N_z) = (90, 30, 60)$, (120, 40, 80) or (160, 50, 100) point grid except for the boundary in the three-dimensional model. The mesh size was $\Delta x = \Delta y = \Delta z = 1R_e$ or $0.6R_e$, and the time step, Δt was selected as $4\Delta x/v_A = 3.7s$ (for $\Delta x = 1R_e$) or $2.25s$ (for $\Delta x = 0.6R_e$) in order to assure that the numerical stability criterion, $v_g^{max}\Delta t/\Delta x < 1$, where v_g^{max} is the maximum group velocity in the calculation domain, was met. Here, the 3-dimensional MHD model was only mentioned, and the 2-dimensional model was not because it is similar to the former. In the latter case, all physical quantities are uniform in the y-direction and a line dipole magnetic field is adopted. The numerical parameters used are mentioned in the following section.

3. Simulation Results

How the magnetospheric configuration responds to the dipole tilt will be demonstrated in the interaction between the solar wind and the magnetosphere by using 2- and 3-dimensional MHD simulations. A snapshot in the quasi-steady state magnetospheric configuration is shown, where the global structure does not change so much. However, for example some small-scale structure of plasma sheet continues to evolve,

for example.

3.1 Two-dimensional simulation result

In the 2-dimensional MHD model we used a $(N_x, N_z) = (200, 100)$ point grid except for the outer boundary in the solar magnetospheric coordinate system and assumed an inclined line dipole magnetic field at the initial state. Moreover, all the physical quantities are uniform in the y-direction. The spatial mesh size was $\Delta x = \Delta z = 2Re$ and the time step, Δt, was chosen as $4\Delta x/v_A = 7.5s$.

The 2-dimensional simulation results of the quasi-steady state magnetospheric configuration on the x-z plane depending on the dipole tilt angle, θ are shown in Figures 1a and 1b, where a snapshot is depicted at 1024 time steps or 128 minutes later in real time. The tilt angles of $\theta = 0°$ and $90°$, respectively, correspond to the north-south direction of the dipole axis and the sunward direction. The left column shows the plasma flow velocity, $\vec{v}$, and the magnetic flux, ψ, by the contours which in fact correspond to the magnetic field lines. The right column shows the plasma pressure by a color code. The formation of the magnetosphere, which is characterized by the bow shock, magnetopause, lobes and plasma sheet, is clearly seen when the solar wind keeps flowing into the simulation box from the left boundary. The parameters of the solar wind are $n_{sw} = 5/cm^3$, $v_{sw} = 300\ km/s$ and $T_{sw} = 2 \times 10^{5o}K$. The plasma sheet and the magnetic neutral sheet for $B_x = 0$ move together toward the northern lobe as the dipole tilt angle increases; in this way the northern edge of the geomagnetic dipole is tilted toward the sun. A new plasma sheet appears from the southern magnetopause for larger tilt angles, and two northern and southern plasma sheets simultaneously exist in the tail. A bumpy structure created in the plasma sheets becomes more remarkable with a larger tilt angle because of the formation of thinner plasma sheets. The plasmoid-like structure in the plasma sheets begins to propagate very slowly down the tail ($v_x = -30\ km/s$). A north-south symmetric magnetosphere with two plasma sheets is again formed for the sunward dipole axis ($\theta = 90°$). The magnetospheric structure for $\theta = 120°$ is the same as that for $\theta = 60°$, when it is inverted. The dependence of the positions of the magnetic neutral sheet for $B_x = 0$ and the magnetopause on the tilt angle, θ, will be discussed later in detail.

3.2 Three-dimensional simulation result

Figures 2a and 2b show the 3-dimensional simulation results of the quasi-steady state magnetospheric configuration on the sun-earth meridian or on the x-z plane, depending on the dipole tilt angle, $\theta = 15° \sim 90°$. In fact, they correspond to a snapshot at 1024 time steps or 64 minutes later in real time. The left column shows the magnetic field where the sunward vector is depicted by the red arrows and the antisunward vector is depicted by the yellow arrows. Therefore, the magnetic neutral sheet must be located between those red and yellow arrows in the noon-

midnight meridian. The right column shows the plasma pressure by color code. The characteristic features of magnetosphere such as the bow shock, magnetopause, lobe and plasma sheet can be clearly recognized. The plasma sheet is naturally located on the solar-magnetospheric equatorial plane for $\theta = 0°$, however the figure is not shown.

The positions of the magnetic neutral sheet and the plasma sheet shift together toward the northern lobe in the tail when the northern edge of the geomagnetic dipole is tilted towards the sun. The plasma sheet expands as the tilt angle, θ, increases from 15° to 45°. In particular, it appears to expand greatly toward the northern magnetopause for $\theta = 45°$, however it is noted later that the northward expansion occurs only near the midnight meridian (see Figure 3). For large tilt angles from $\theta = 60°$ to 90°, the plasma sheet shifts more northward and simultaneously becomes narrower. Then another plasma sheet appears from the southern magnetopause. As a two-fold result, two plasma sheets exist at the same time on the midnight meridian for $\theta \geq 45°$, and symmetric twin plasma sheets are formed for $\theta = 90°$, in which the dipole axis points to the sun. It can be found later that the plasma sheet in fact forms a ring in the tail cross section. Moreover, it is noted that a bumpy structure appears in the thinner plasma sheet for $\theta = 60° \sim 90°$. The plasmoid-like structure slowly propagates down the tail as time elapses.

In Figures 3a and 3b are shown the plasma pressures, p in the tail cross section at three different positions of $x = -15.5$, -30.5 and $-45.5Re$ for seven tilt angles from $\theta = 0°$ to 90°. Then, the x-component of the magnetic field, B_x, in the tail cross section is also shown in Figures 4a and 4b in the same condition, where the blue shows the positive B_x of earthward component and the red the negative B_x of tailward component. The patterns of p and B_x clearly indicate the formation of the plasma sheet, and the two northern and southern lobes. The neutral sheet should be located at the boundary between the positive B_x (red part) and the negative B_x (blue part).

The plasma sheet and the magnetic neutral sheet corresponding to $B_x = 0$, which are formed on the solar magnetospheric equatorial plane for $\theta = 0°$, are raised above it near the midnight meridian and show an arched shape in the tail cross section for $\theta > 0°$. The tendency is a little stressed in distant tail. Both shift toward the northern lobe near the midnight meridian for $\theta > 0°$, but then shift oppositely and southward near the flanks of the magnetopause. Thus, the plasma sheet and the magnetic neutral sheet are raised above the GSM equatorial plane around the local midnight and are depressed from it near the flanks, when the northern edge of the geomagnetic dipole is tilted toward the sun. These features are consistent with the previous observations of *Fairfield* [1980] and *Gosling et al.* [1986]. One of the interesting features of the simulation is that the plasma sheet simultaneously expands southward near the midnight meridian (see the plasma pressure pattern for $\theta = 15° \sim 60°$), when the central part of the plasma sheet shifts toward the northern lobe. The plasma sheet forms an arched shape and also directs its tongue southward.

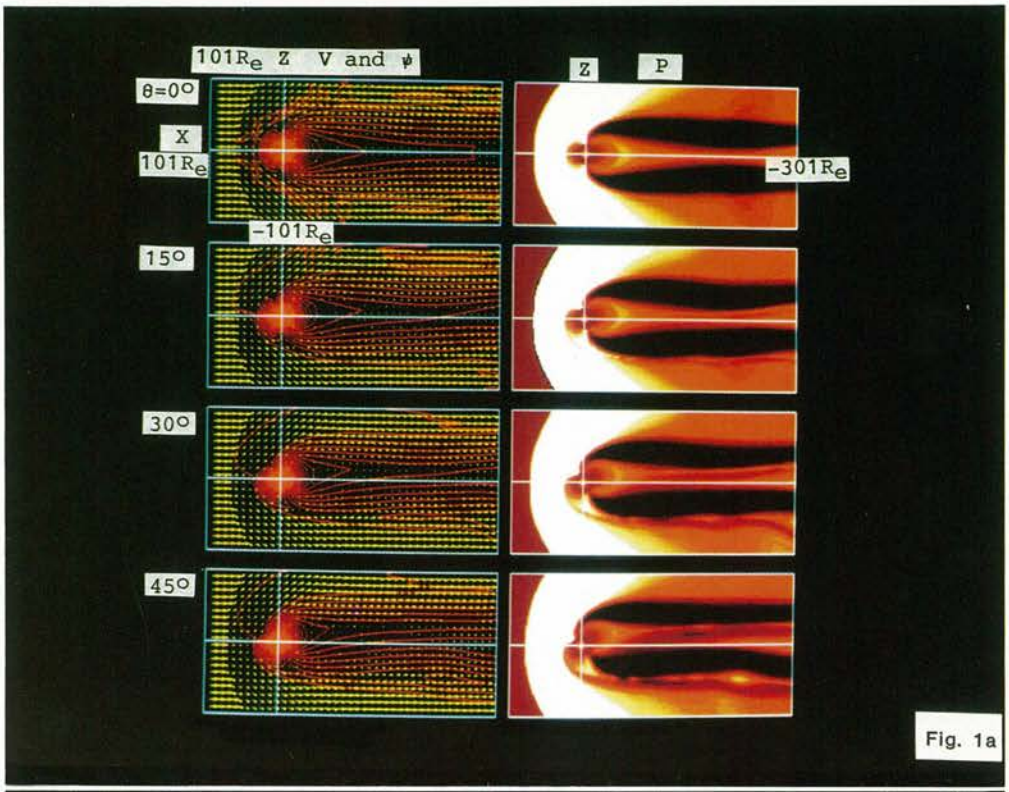

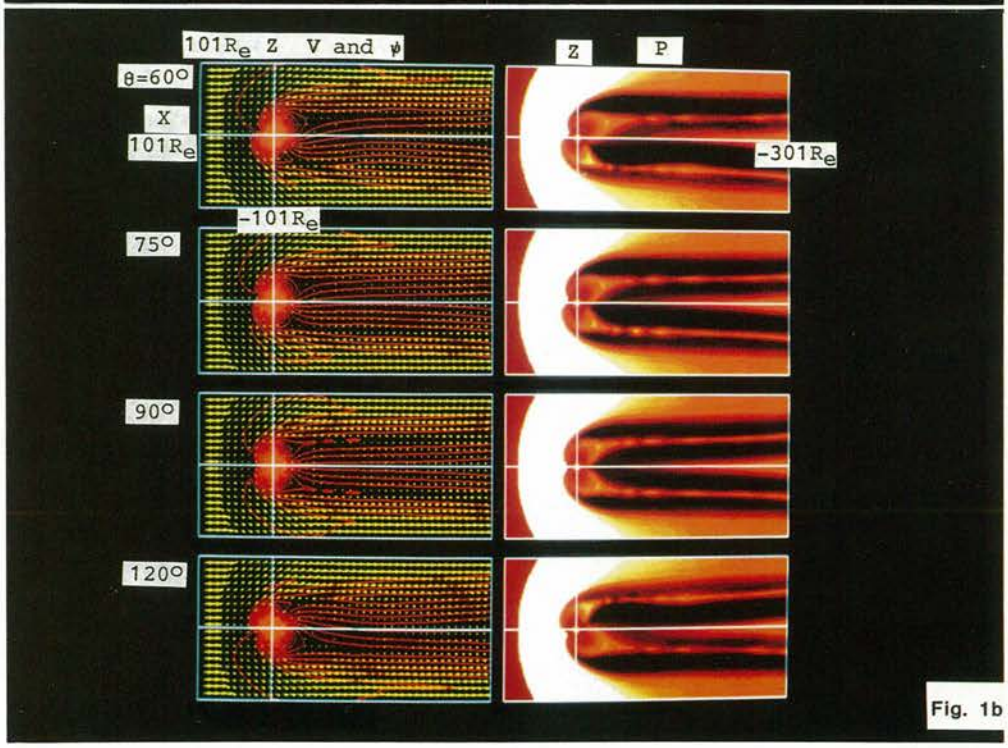

Fig. 1a. and 1b. Two-dimensional MHD simulation result of the quasi-steady state magnetospheric configuration depending on the dipole tilt angles, $\theta = 0° \sim 120°$.

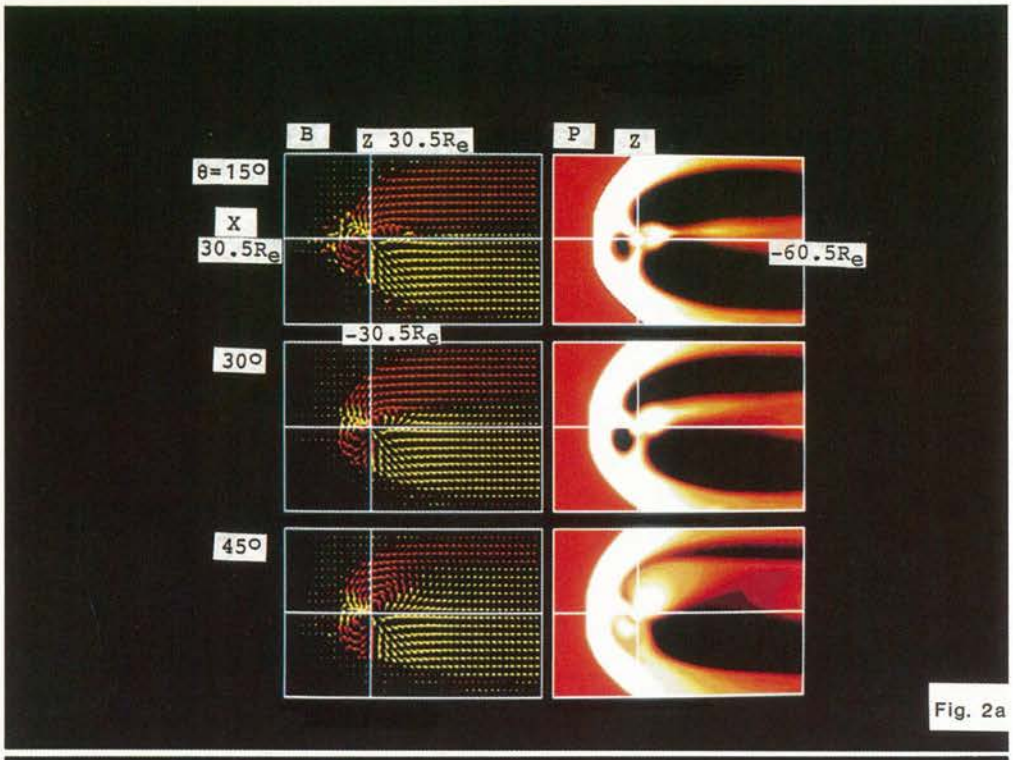

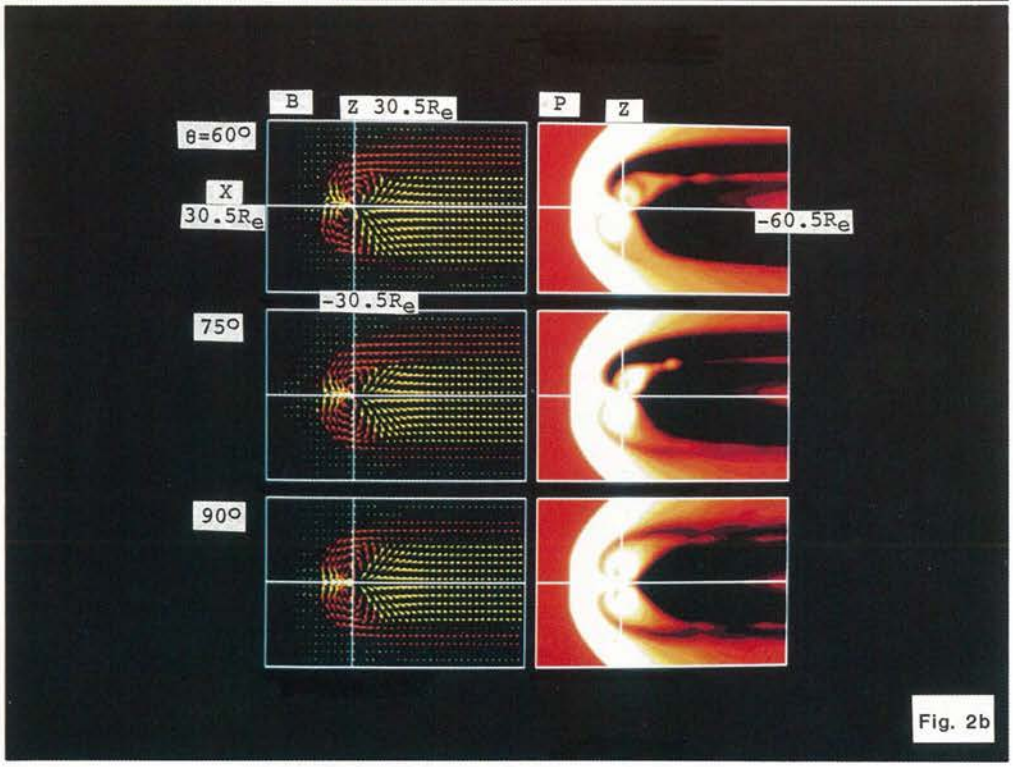

Fig. 2a. and 2b. Three-dimensional MHD simulation result of the quasi-steady state magnetospheric configuration in the sun-earth meridian depending on the dipole tilt angles, $\theta = 15° \sim 90°$.

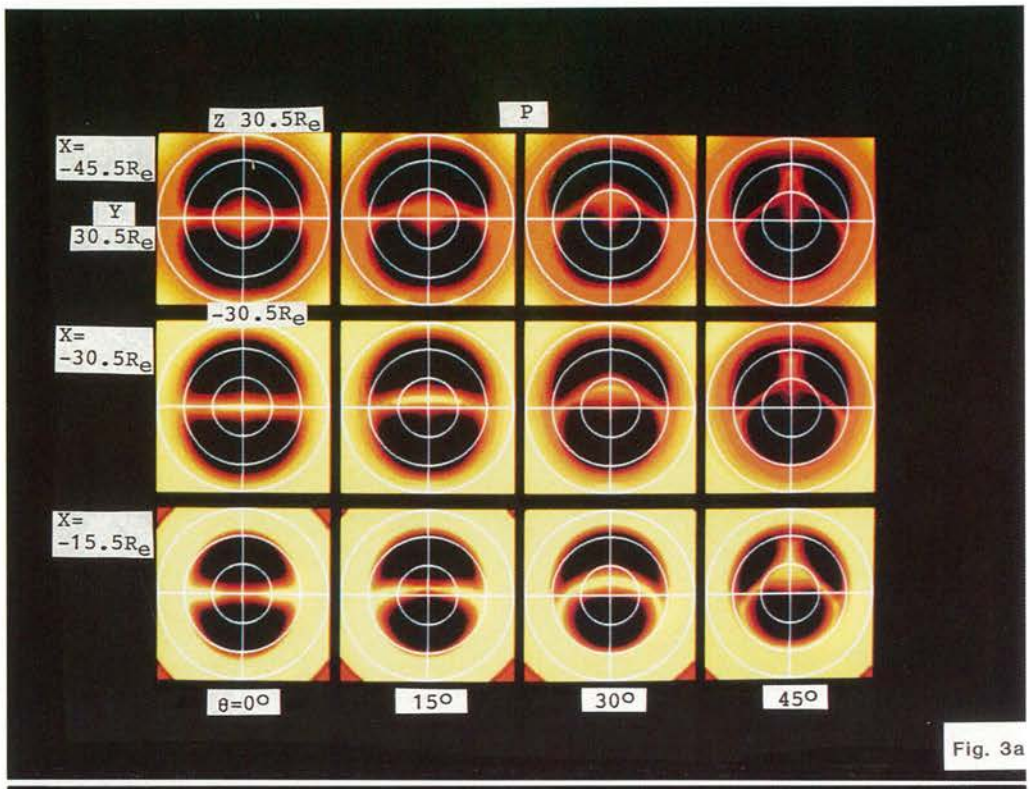

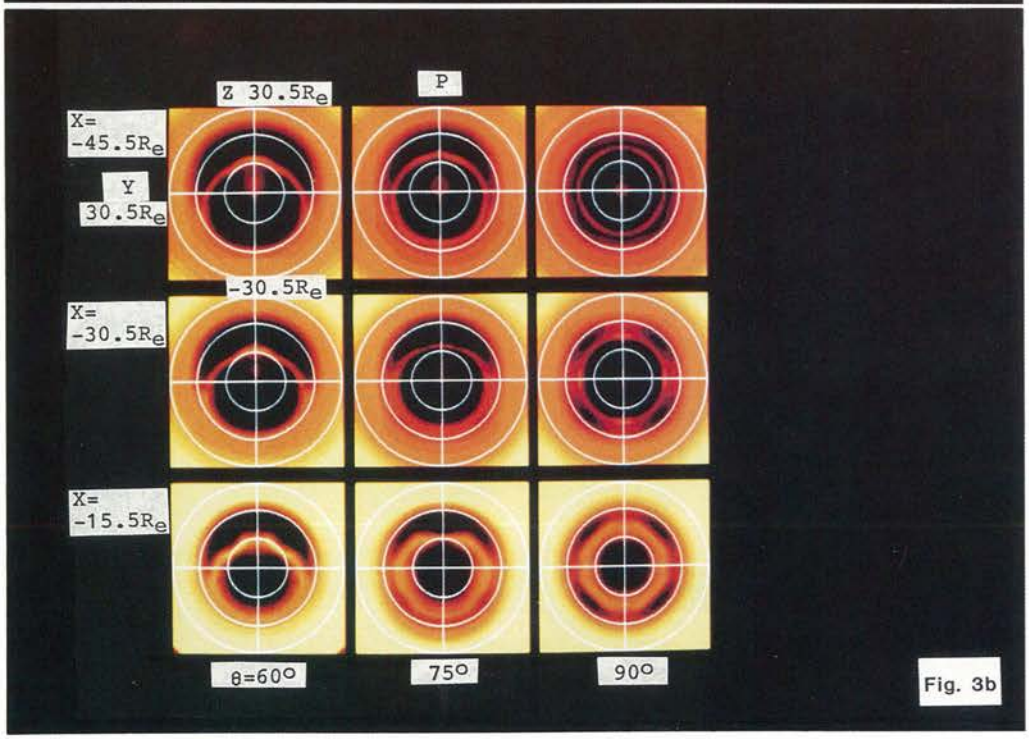

Fig. 3a. and 3b. Structure of the plasma sheet in the tail cross section depending on the dipole tilt angles, $\theta = 0° \sim 90°$, where the plasma pressure is depicted by color code.

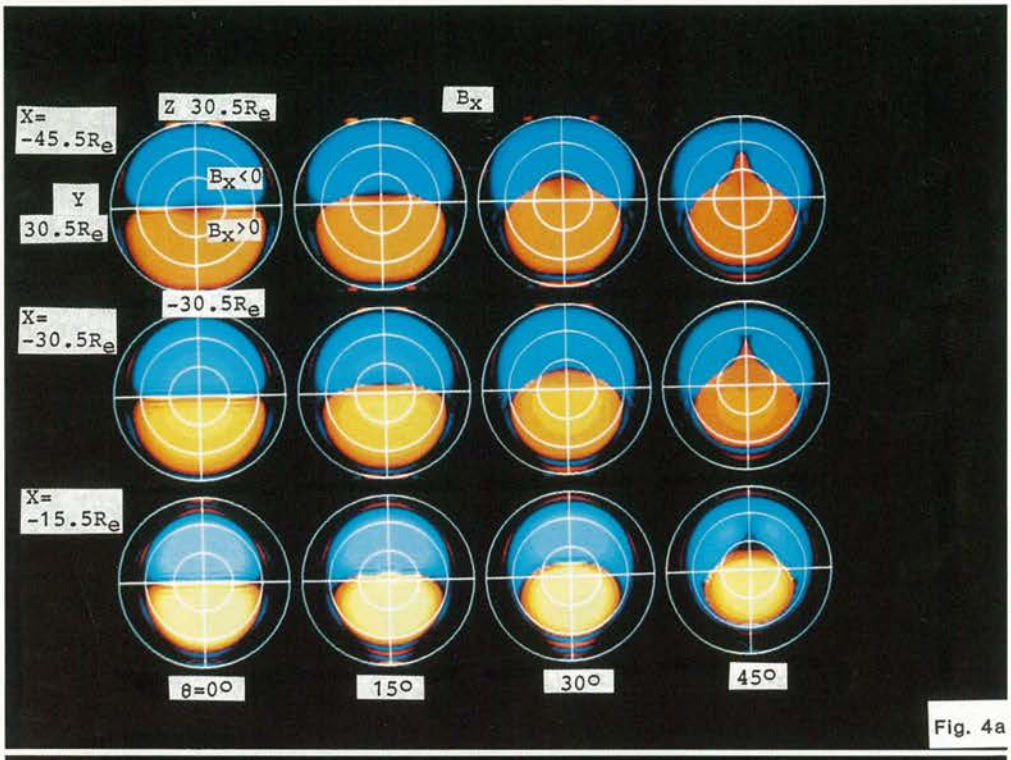

Fig. 4a

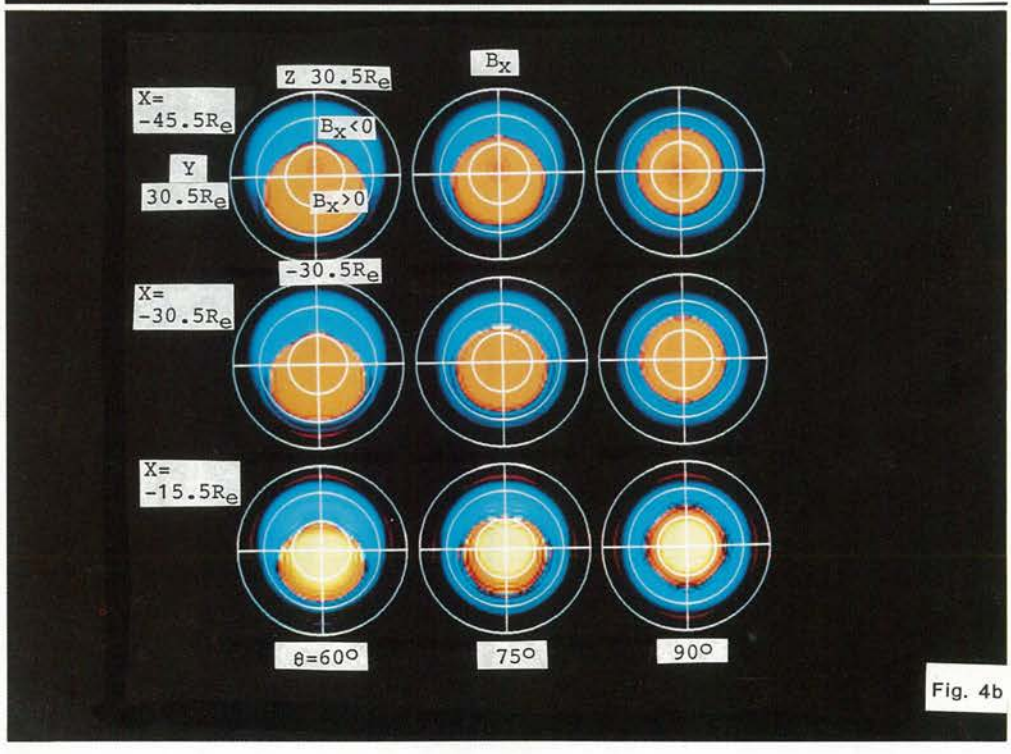

Fig. 4b

Fig. 4a. and 4b. Configuration of the x-component of magnetic field, B_x in the tail cross section depending on the tilt angles, $\theta = 0° \sim 90°$ where the positive B_x (sunward vector) is depicted by the red and the negative B_x (tailward vector) is depicted by the blue.

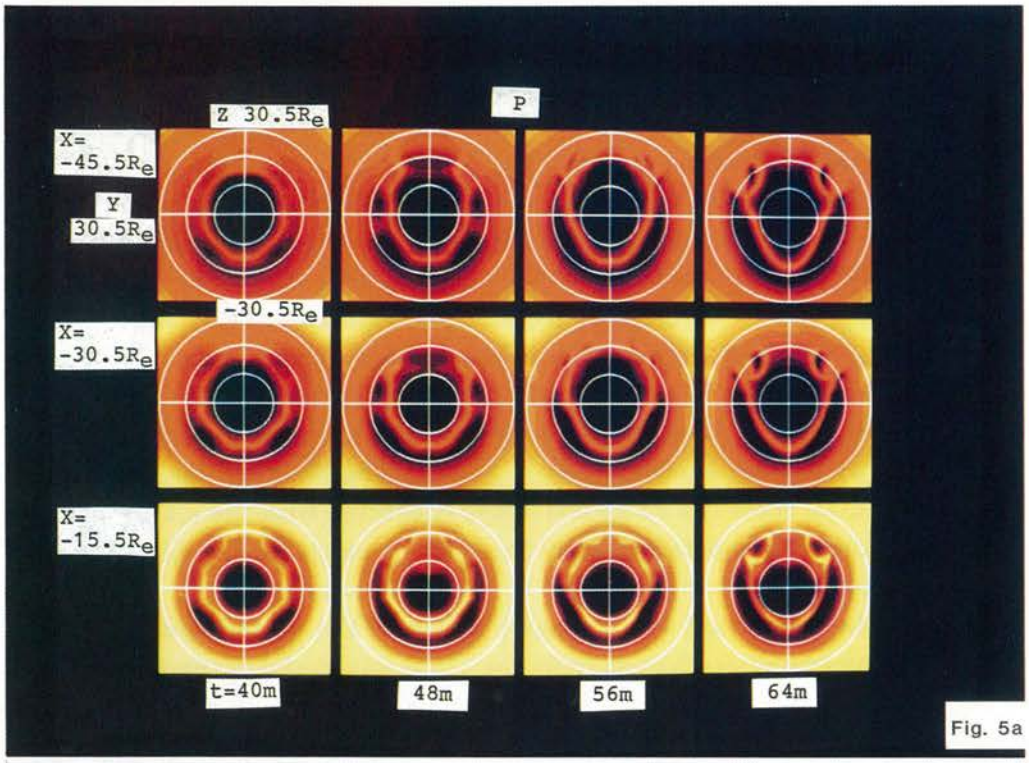

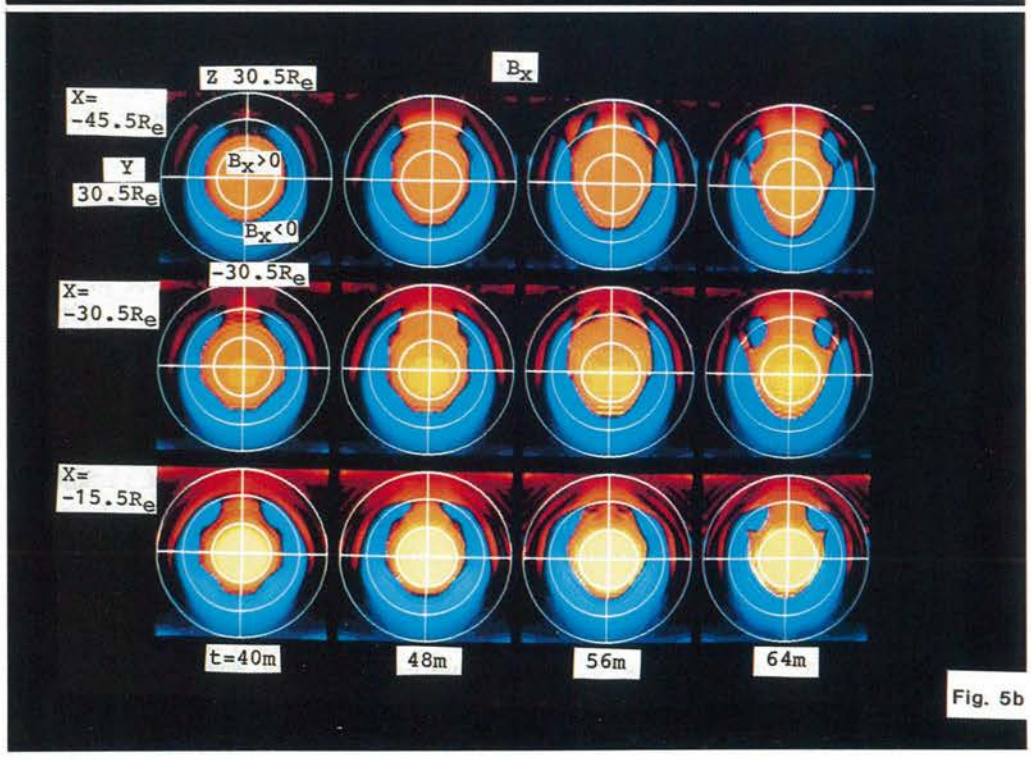

Fig. 5a. and 5b. Time evolution of the magnetotail configuration when a uniform northward IMF of $B_z = 5nT$ begins to flow with the solar wind and interacts with the quasi-steady state magnetosphere for the tilt angle of $\theta = 90°$, where the patterns of p (5a) and B_x (5b) are depicted by the color code.

For $\theta = 45°$, the plasma sheet extends greatly toward the northern magnetopause near the midnight meridian (compare with Figure 2a for $\theta = 45°$), and a horn of the tailward magnetic field intrudes into the northern lobe there on the B_x pattern. This strange plasma sheet expansion will need a further study and might be partly associated with the limit of the grid spacing.

The arched shape of plasma sheet is more distinguishable for larger tilt angle. The plasma sheet forms an oval detached from the magnetosheath in the tail cross section for $\theta = 60°$ and $75°$, and it eventually forms a ring for $\theta = 90°$. The transformation can be clearly seen on the B_x pattern. The magnetic neutral sheet for $B_x = 0$ is located on the boundary between the tailward magnetic field depicted by the red and the earthward field by the blue as was previously mentioned. The region of the tailward magnetic flux is almost surrounded by that of the earthward magnetic flux for $\theta = 45°$. The feature is obvious for $\theta \geq 60°$. Therefore we can conclude that the magnetic neutral sheet has an arched shape connected with the magnetopause for $\theta \leq 30°$ and an oval-shape detached from the magnetopause for $\theta \geq 45°$. The critical angle is suggested to be about $\theta = 30° \sim 45°$ from the simulation.

It should be noted that the average position of the magnetopause on the B_x pattern shifts somewhat northward from the GSM equatorial plane for $\theta = 15° \sim 75°$. For example, the position of the magnetopause at the midnight meridian is $z = -24Re$ at $x = -30.5Re$ in the southern hemisphere, while $z = 28Re$ in the northern hemisphere for $\theta = 30°$. This is because the nightside magnetic flux of the tilted geomagnetic dipole slightly pushes up the entire magnetotail.

3.3 Magnetotail dynamics in effect of IMF

In Figures 5a and 5b is shown a time evolution of the magnetotail configuration when a uniform northward IMF of $B_z = 5nT$ begins to flow into the simulation box with the solar wind and interacts with the quasi-steady magnetospheric configuration for $\theta = 90°$, which is shown in Figure 2, 3 and 4. The time is measured from the switching on the northward IMF. The plasma sheet, which initially forms a ring in the tail cross section for $\theta = 90°$, is broken in the northern part and merges into the hot plasma of the northern magnetosheath. This is because the magnetic reconnection begins to occur on the northern magnetopause where the antiparallel field condition is satisfied between the tilted dipole field for $\theta = 90°$ and the draped IMF. On the B_x pattern, the area of the tailward magnetic flux depicted by the red, which is initially surrounded by that of the earthward flux, extends toward the northern lobe and merges with that of the tailward magnetic flux created by the draped northward IMF. At the same time a fine structure like arcs appears for p and B_x in the region in which the magnetic reconnection is occurring. The magnetotail dynamics in the simulation suggests that the plasma sheet (or plasma oval), when detached from the magnetosheath for a large tilt angle can be mixed with the magnetosheath plasma by the magnetic reconnection process, reflecting the possibly very dynamic behavior in

the interaction process.

4. Model of Neutral Sheet

A simple analytical model will be proposed in order to explain the position and the shape of the magnetic neutral sheet for $B_x = 0$ (or magnetic neutral sheet), which was demonstrated by the MHD simulation. The main purpose is to obtain a basic model of the magnetic neutral sheet which is applicable for all dipole tilt angles.

For the first time we will make two important assumptions to obtain a magnetic neutral sheet model. The first is that the neutral sheet is raised (or depressed) to the height above (or below) the GSM equatorial plane, where the height is given by the point on the line with a half angle of the dipole tilt at a distance close to the magnetopause in the tail (see Figure 6). The second is that the area of the tailward magnetic flux equals that of the earthward magnetic flux in the tail cross section. The neutral sheet is raised along the magnetic equator near the earth ($r \leq 8Re$), yet has a gentle gradient and becomes flatter near the hinging distance in the tail as shown in Figure 6. Therefore, we can expect the first assumption, in which the angle for the tailward magnetic flux equals that for the earthward magnetic flux in the arc between the GSM north pole and the geomagnetic south pole at the distance close to the magnetopause, when the northern edge of the geomagnetic dipole is tilted toward the sun. Thus it can be understood that the first assumption really comes from a physical idea similar to the second one and determines the feature of the transition.

In Figure 7 are shown the two- and three- dimensional models of the position of the magnetic neutral sheet in the midnight meridian in the far tail for all the dipole tilt angles, θ, where the distance of the magnetopause is assumed to be constant. In the 2-dimensional model, the circle corresponds to the distance to the magnetopause, r_0. The position of the neutral sheet in the northern hemisphere can be determined as $z = r_0 \sin(\theta/2)/(1 + \sin(\theta/2))$ in that case by the intersection between the two lines of $z = r_0 + x$ and $z = -x \sin(\theta/2)$ in the solar magnetospheric coordinate system for $0° \leq \theta \leq 90°$. Moreover, the position of the neutral sheet in the southern hemisphere is given by $z = -r_0/(1 + \sin(\theta/2))$ according to the second requirement. The relationship can be applied for all the dipole tilt angle when the symmetry is taken into account. It is noted that the positions of the neutral sheet are $z = \pm r_0/2$ for $\theta = 90°$.

In the 3-dimensional model, the position of the neutral sheet of the northern hemisphere on the midnight meridian can be determined as $z = r_0 \sin(\theta/2)$ by the intersection between the circle of $x^2 + z^2 = r_0^2$ and the line of $z = -x \tan(\theta/2)$ for $0 \leq \theta \leq 90°$ in the solar magnetospheric coordinate system. The position of the neutral sheet in the southern hemisphere can be determined by the requirement for

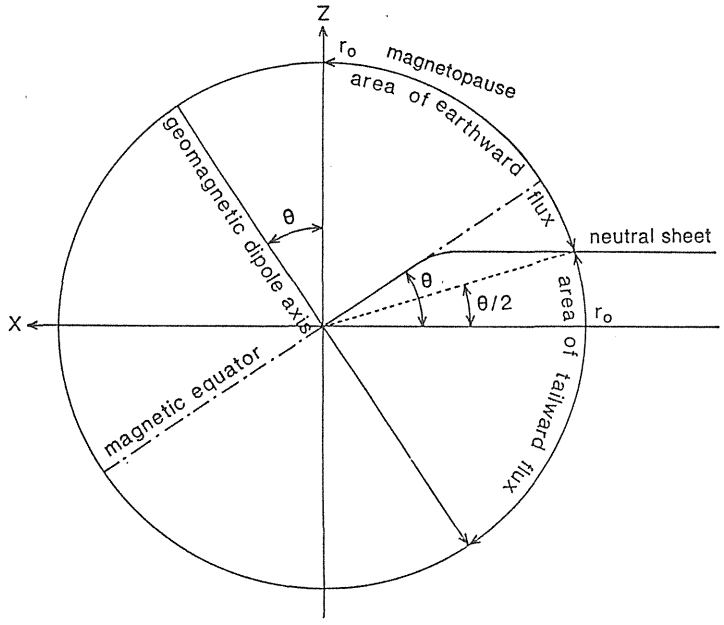

Fig. 6. Schematic diagram of the relationship between the dipole tilt and the magnetic neutral sheet for $B_x = 0$. The magnetic neutral sheet is assumed to be elevated in height for a half the dipole tilt angle at a distance close to the magnetopause in the tail.

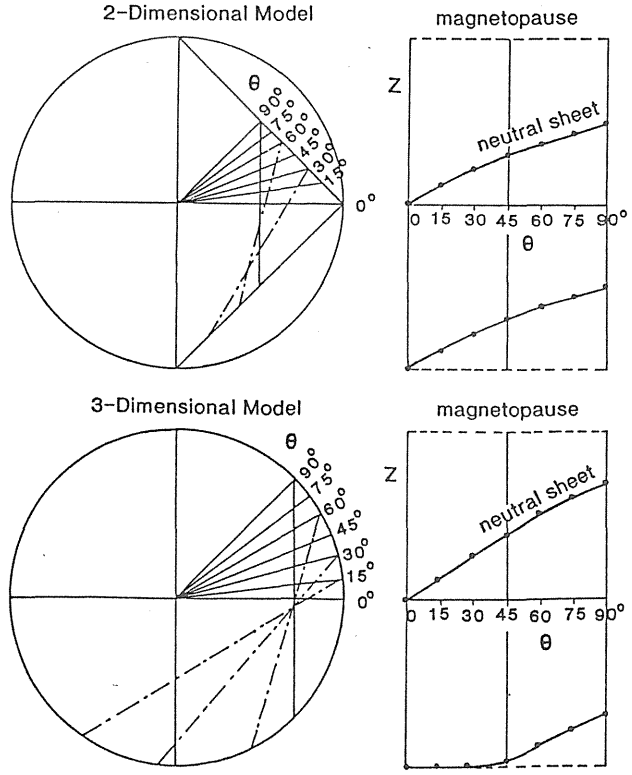

Fig. 7. Two- and three-dimensional models of the position of the magnetic neutral sheet on the midnight meridian for all the dipole tilt angle, θ.

the second assumption.

In order to obtain the shape of the magnetic neutral sheet in 3 dimensions, let us consider a sphere with the radius of the magnetopause described by $x^2+y^2+z^2=r_0^2$ and a plane described by $z-r_0\sin(\theta/2)=-\tan\alpha(x+r_0\cos(\theta/2))$, where α is some angle of the plane in relation to the GSM equatorial plane and can be determined by the second assumption. Inserting the plane equation of $x=-z\cot\alpha-x_1$ into the spherical equation, we obtain the following elliptic equation for the neutral sheet from the intersection on the y-z plane,

$$\frac{(z+z_1)^2}{a^2}+\frac{y^2}{b^2}=1 \tag{1}$$

where

$$a=r_0\sin\alpha\cos(\alpha-\frac{\theta}{2}), \qquad b=r_0\cos(\alpha-\frac{\theta}{2})$$
$$z_1=r_0\cos\alpha\sin(\alpha-\frac{\theta}{2}) \quad and \quad x_1=r_0\sin(\alpha-\frac{\theta}{2})/\sin\theta.$$

There are two cases, depending on whether or not the bottom of the oval is located in the region for $x>0$. The necessary critical condition is given by inserting $z=-r_0$ snd $y=0$ into (1) as

$$\sin(2\alpha-\frac{\theta}{2})=1 \tag{2a}$$

or

$$2\alpha-\frac{\theta}{2}=\frac{\pi}{2} \tag{2b}$$

On the other hand, the area of the oval in (1), which corresponds to the region of the tailward magnetic flux, is easily calculated as

$$S_1=\pi ab \tag{3}$$

The second assumption of $2S_1=S_0\equiv\pi r_0^2$ is reduced to the following expression,

$$2\sin\alpha\cos^2(\alpha-\frac{\theta}{2})=1 \tag{4}$$

when the bottom of the ellipse is located in the nightside for $x<0$. Inserting (2b) into (4), the critical angle can be determined by the following relationship,

$$\sin^3\alpha=\frac{1}{2} \tag{5}$$

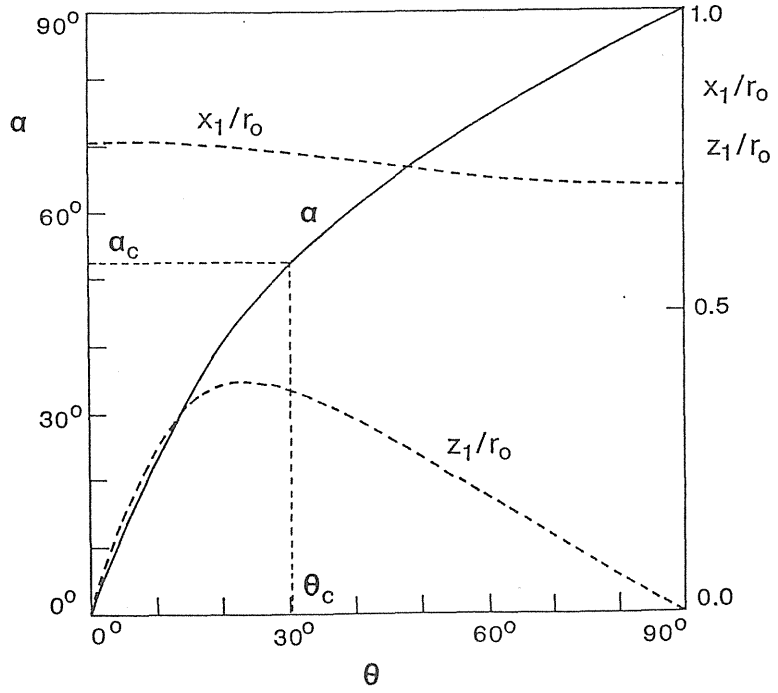

Fig. 8. Dependence of α, x_1/r_0 and z_1/r_0 on the dipole tilt angle, θ, when the area of the tailward magnetic flux equals that of the earthward flux.

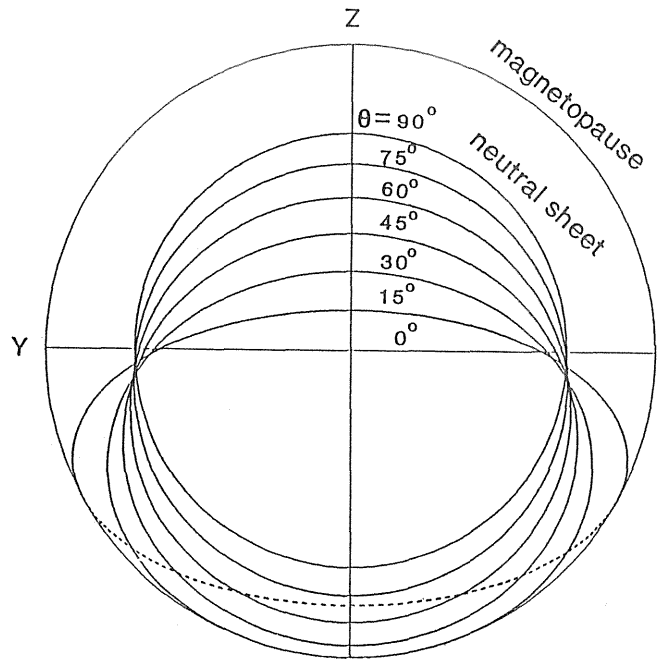

Fig. 9. Three-dimensional model of the shape of the magnetic neutral sheet for $B_x = 0$ in the tail cross section for several dipole tilt angles, θ, where the magnetopause is assumed to be a constant circle.

as $\alpha_c = 52.53°$ and $\theta_c = 30.13°$. Therefore the shape of the magnetic neutral oval is described by (1) and (4) in the tail cross section for $\theta_c \leq \theta \leq 90°$. The position of the northern neutral sheet is given by $z = r_0 \sin(\theta/2)$ in the midnight meridian; that of the southern neutral sheet is given by $z = -r_0 \sin(2\alpha - \theta/2)$. Therefore, the positions of the neutral sheet are $z = \pm r_0/2^{1/2}$ in the midnight meridian for $\theta = 90°$.

When the dipole tilt angle, θ, is less than the critical angle, θ_c, the area of the tailward magnetic flux, S_2, should be encompassed by the upper part of the oval in (1) and the lower part of the magnetopause circle described by $y^2 + z^2 = r_0^2$ on the y–z plane. The tangential point of the two curved lines is given by $z = z_2 = -r_0 \sin(\alpha - (\theta/2))/\cos\alpha$, and the area of the tailward magnetic flux is calculated as

$$\begin{aligned}\frac{1}{2}S_2 &= \int_{-r_0}^{z_2} dz(r_0^2 - z^2)^{1/2} + \int_{z_2}^{z_3} dz \frac{b}{a}\{a^2 - (z + z_1)^2\}^{1/2} \\ &= [z(r_0^2 - z^2)^{1/2} + r_0^2 \sin^{-1}(z/r_0)]_{-r_0}^{z_0} \\ &\quad + \frac{b}{a}[z(a^2 - z^2)^{1/2} + a^2 \sin^{-1}(z/a)]_{z_2+z_1}^{z_3+z_1} \qquad (6)\end{aligned}$$

where $z_3 = -z_1 + a$. Therefore, the second requirement can be satisfied by the following relationship,

$$2S_2 = S_0 = \pi r_0^2 \qquad (7)$$

As a result, the shape of the magnetic neutral sheet for $B_x = 0$ is obtained by (1) and (7) in the tail cross section for $0 \leq \theta \leq \theta_c$. The position of the magnetic neutral sheet on the midnight meridian is shown in Figure 7 for $0° \leq \theta \leq 90°$.

The dependences of α, x_1/r_0 and z_1/r_0 on the dipole tilt angle, θ, are shown in Figure 8 when the relationship in (4) or (7) is satisfied. An approximate expression of $\alpha = (1 + 1/2^{1/2})\theta$ is valid for small θ. Moreover, $\alpha = \alpha_c$ is valid for $\theta = \theta_c$ and then $\alpha = 90°$ for $\theta = 90°$.

In Figure 9 is shown the shape of the magnetic neutral sheet in the tail cross section for several dipole tilt angles of $\theta = 0° \sim 90°$, where the magnetopause is simply assumed to be a circle. The dashed line means the dayside neutral sheet for $\theta < \theta_c$ and does not appear in the tail. The neutral sheet with an arched shape is over the solar magnetospheric equatorial plane near the midnight meridian and below it on the flanks of the magnetopause for $\theta < \theta_c$. On the other hand, it forms an oval detached from the magnetopause for $\theta > \theta_c$ and becomes a ring for $\theta = 90°$.

When the format of the empirical magnetic neutral sheet model for $B_x = 0$ by Fairfield [1980] is adopted, (1) can be rewritten as

$$\begin{aligned}z &= a(1 + \frac{y^2}{b^2})^{1/2} - z_1 \\ &= \{(H_0 + D)(1 - \frac{y^2}{Y_0^2})^{1/2} - D\}\sin\theta \qquad (8)\end{aligned}$$

where

$$D = r_0 \frac{\cos\alpha \sin(\alpha - \theta/2)}{\sin\theta}, \qquad Y_0 = r_0 \cos(\alpha - \theta/2)$$

$$H_0 + D = r_0 \frac{\sin\alpha \cos(\alpha - \theta/2)}{\sin\theta} \quad and \quad H_0 = \frac{r_0}{2\cos(\theta/2)}$$

These parameters can be approximated as $D = r_0(1 + 2^{1/2})/2$, $Y_0 = r_0$ and $H_0 = (1/2)r_0$ from $\alpha = (1+1/2^{1/2})\theta$ for $\theta << 1$ and then as $D = 0.740r_0$, $Y_0 = 0.794r_0$ and $H_0 = 0.528r_0$ for the critical angle of $\theta = \theta_c = 30.13°$. In these parameters, the value of D seems to be particularly larger than that given by *Fairfield* [1980] or *Gosling et al.* [1986]. However, the present neutral sheet model is only a little different from that of the empirical model, because an oval neutral sheet is adopted here for all the dipole tilt angles. In fact, the present neutral sheet model gives a result similar to the empirical model, except for near the magnetopause, for a tilt angle smaller than the critical angle.

5. Discussion

For the first time the simulated position of the magnetic neutral sheet for $B_X = 0$ in the midnight meridian will be compared with the position given by the present theoretical model of the neutral sheet. In Figure 10 is shown the dependence of the positions of the magnetopause and the neutral sheet on the dipole tilt angle, θ, for the 2-dimensional case. The upper panel directly shows the simulated positions of the magnetopause and the neutral sheet versus θ. The MHD simulations were practically executed for the tilt angle between $\theta = 0°$ and 90°. However, the plots in Figure 10 are depicted for the complete range of the tilt angle by the consideration of symmetry to clearly show the dependence of the positions of the magnetopause and neutral sheet on the tilt angle. The magnetopause shrinks for $\theta = 0°$ down to 0.76 times the maximum distance for $\theta = 90°$, even though the magnetic pressure of the 2-dimensional line dipole is isotropic. It is noted that the neutral sheet seems to virtually coincide with that of the magnetopause at $\theta = 0°$, a feature slightly different from the 3-dimensional result (compare with Figure 11).

In the lower panel the position of the simulated neutral sheet (open circles), which is normalized to the distance of the magnetopause, is compared with that of the 2 dimensional neutral sheet model (solid line). There is quite good agreement between the results from the simulation and the 2-dimensional model.

In Figure 11 is shown the dependence of the positions of the magnetopause and the neutral sheet in the midnight meridian on the dipole tilt angle, θ, for the 3-dimensional case. The format of the figure is same as for the 2-dimensional case in Figure 10. The simulated position of the magnetopause as well as that of the neutral

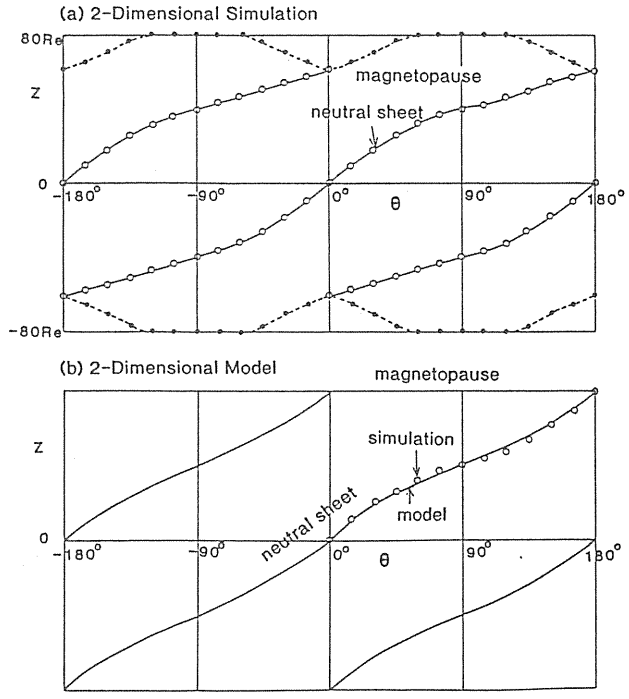

Fig. 10. Dependence of the positions of the magnetopause and the neutral sheet for $B_x = 0$ on the dipole tilt angle, θ, in the 2-dimensional case.

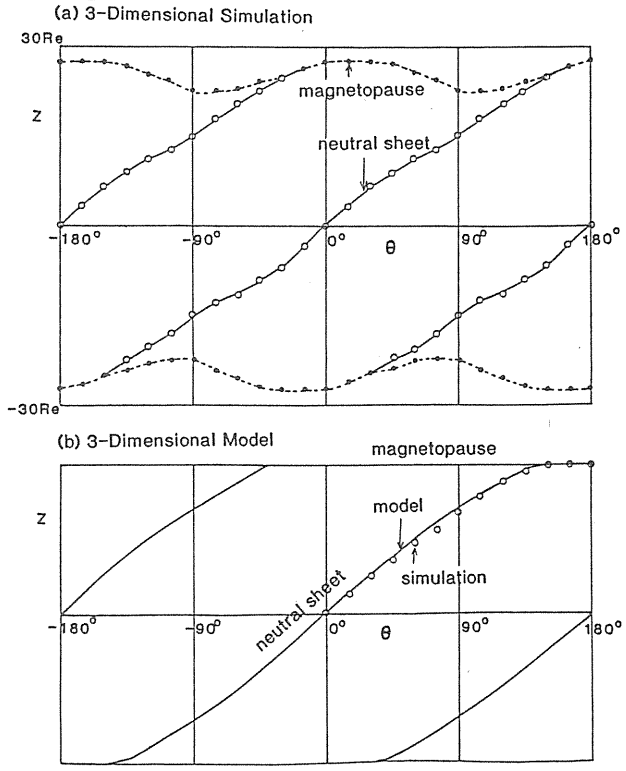

Fig. 11. Dependence of the positions of the magnetopause and the neutral sheet for $B_x = 0$ in the midnight meridian on the dipole tilt angle, θ, in the 3-dimensional case.

sheet changes depending on the tilt angle, θ, in the upper panel. The magnetopause expands in the midnight meridian for $\theta = 0°$ and shrinks for $\theta = 90°$ down to 0.82 times the maximum distance. This tendency seems to be opposite that for the 2-dimensional case, while the magnetic pressure of the 3-dimensional dipole on the dipole axis is 4 times stronger than that on the magnetic equator at the same distance. The simple pressure balance gives the ratio of the magnetopause distance for $\theta = 90°$ to be 0.97-fold that for $\theta = 0°$. Therefore, the magnetopause tends to expand more for $\theta = 90°$ than the case when the pressure balance is simply taken into account. It is noted that the neutral sheet virtually coincides with the magnetopause line near $\theta = \pm 30°$. This feature differs from the 2-dimensional result (see Figure 10), which is very consistent with the existence of the critical angle $\theta_c = 30.13°$ in the 3-dimensional magnetic neutral sheet model. And a north-south asymmetry can be seen between the northern and southern parts of the magnetopause (compare with Figure 4).

In the lower panel the position of the simulated neutral sheet (open circles), which is normalized to the distance of the magnetopause, is compared with that of the 3-dimensional neutral sheet model (solid line). There is again good agreement between the simulation result and the 3-dimensional model. Also, the simulated shape of the magnetic neutral sheet in the tail cross section in Figure 4 is quite similar to the shape of the neutral sheet model in Figure 9 even near the magnetopause.

When the present simulation results and neutral sheet model are compared with the empirical neutral sheet model by *Fairfield* [1980] and *Gosling et al.* [1986], the general tendency of the neutral sheet is very similar for a small dipole tilt angle and shows no appreciable quantitative difference for the most part. However, there exist small differences. One is that both the simulated and model neutral sheets are somewhat above that of the empirical model for $\theta = 30°$ when the neutral sheets in Figure 9 are compared with those in Figure 6 of the paper by *Gosling et al.* [1986]. Another is that the present neutral sheet is smoothly connected with the magnetopause by a tangential line. The tangential connection of the neutral sheet seems to be physically more favorable in the ideal steady magnetosphere when the draped magnetic field lines are considered near the magnetopause. However, the position and the shape of the magnetic neutral sheet can be easily deviated and frequently modified from the quasi-steady state configuration because the real magnetotail is more dynamic and must undergo the influence of the IMF.

The critical angle in which the neutral sheet is tangential to the magnetopause was suggested by *Siscoe* [1971] as a transition from the earth-like neutral sheet to a closed cylindrical neutral sheet for the tilt angle of $\theta = 90°$. The magnetotail configuration for such a critical angle was also demonstrated from an approximate MHD equilibrium calculation for $\theta = 45°$ by *Voigt et al.* [1983]. The present simulation result of the plasma sheet in Figure 3 is similar to their equilibrium configuration. We suggested the critical angle of $\theta_c = 30.13°$ which somewhat differs from the $\theta = 45°$ chosen by *Voigt et al.* Still, it may be better to say that the critical angle is around

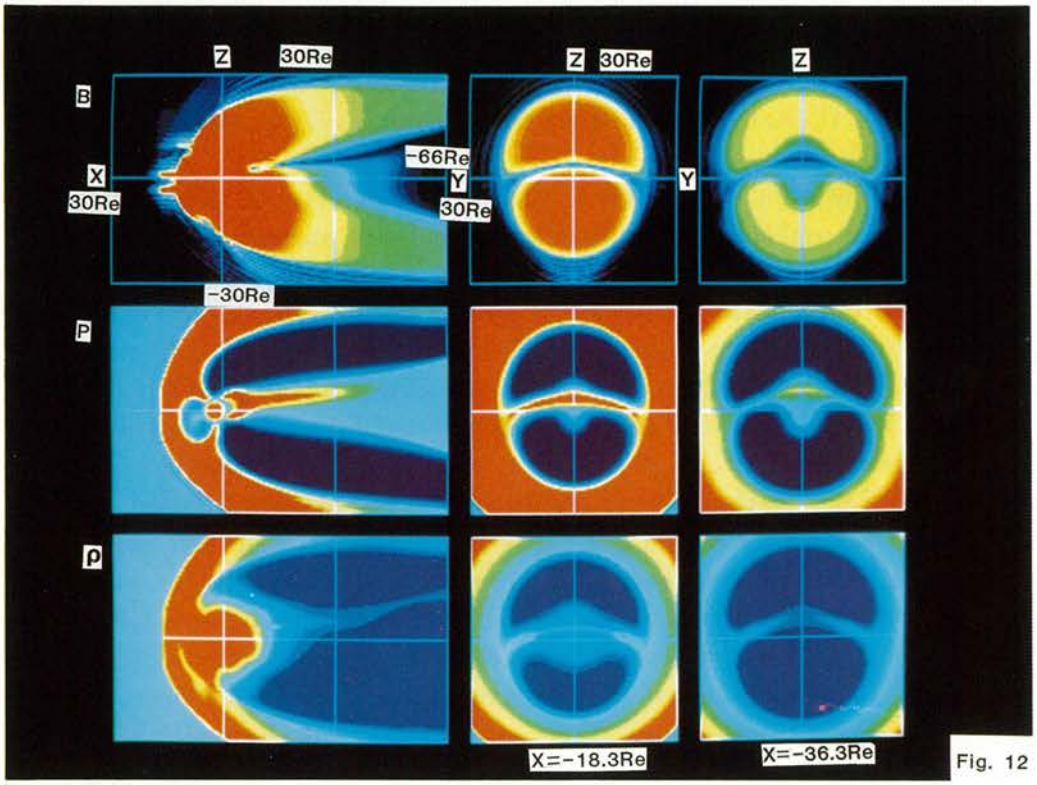

Fig. 12. Configuration of the plasma density, ρ, the plasma pressure, p, and the magnitude of magnetic field, B, on the noon-midnight meridian and their cross sectional patterns at $x = -18.3Re$ and $-36.3Re$ in the tail for the dipole tilt angle of $\theta = 20°$, where a $(N_x, N_y, N_z) = (160, 50, 100)$ point grid is used with the grid spacing of $\Delta x = \Delta y = \Delta z = 0.6Re$.

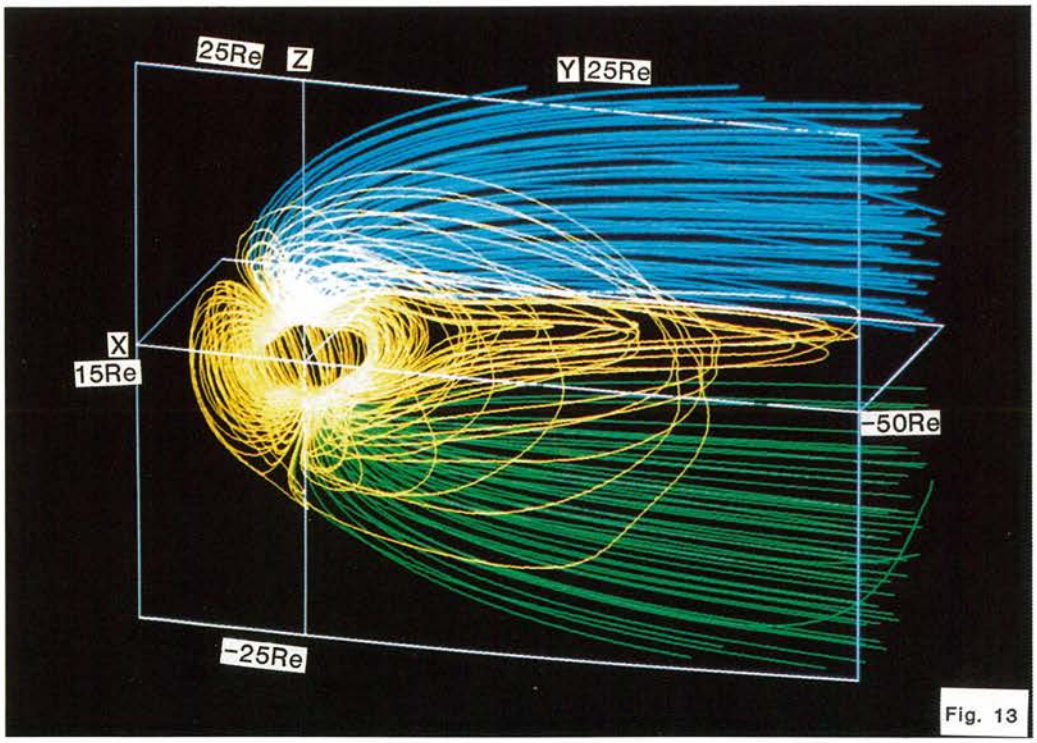

Fig. 13. Three-dimensional configuration of the magnetic field lines for $\theta = 20°$ in the same calculation as in Figure 12.

$\theta = 30° \sim 45°$ because the transition from $\theta = 30°$ to $45°$ in the simulation is very gentle (see Figure 4). And also there is no observational evidence for a detailed plasma sheet at the earth.

By using the simulation result of the interaction between the solar wind and the earth's magnetosphere with higher spatial resolution and a typical tilt angle, the effect of dipole tilt will be discussed in more detail. In Figure 12 are shown the configuration of the plasma density, ρ, the plasma pressure, p, and the magnitude of magnetic field, B, on the noon-midnight meridian and their cross sectional patterns at $x = -18.3Re$ and $-36.3Re$ in the tail for the dipole tilt angle of $\theta = 20°$, where a $(N_x, N_y, N_z) = (160, 50, 100)$ point grid is used except for the boundary and the grid spacing is selected as $\Delta x = \Delta y = \Delta z = 0.6Re$. The magnetic neutral sheet is above the GSM equatorial plane in the central plasma sheet region and below it near the magnetopause as was previously mentioned. The neutral sheet and the maximum pressure of plasma sheet form an arch shape in the tail cross section, and at the same time the plasma sheet also expands toward the southern lobe near the midnight meridian. The plasma sheet forms an arch and also puts out its tongue into the southern lobe. The thickness of the central plasma sheet itself decreases in the distant tail, whereas the thickness of the expanded plasma sheet region with lower plasma pressure tends to increase down the tail. Moreover, the whole magnetotail somewhat shifts toward the north for $\theta = 20°$. The magnetopause somewhat expands in the northern part but shrinks in the southern part when the northern edge of geomagnetic dipole is tilted toward the sun (positive tilt).

In Figure 13 is shown the 3-dimensional configuration of the magnetic field lines for $\theta = 20°$ in the same calculation as in Figure 12. The yellow shows the closed field lines, while the blue and the green show the open field lines which have their footpoints on the northern and southern ionospheres, respectively. Convex and largely rounded yellow lines correspond to the traveling magnetic field lines near the magnetopause from dayside to nightside. These field lines can dominantly control the structure of the depressed neutral sheet on flanks of the magnetopause. The narrow closed tail field lines are above the GSM equator for $\theta = 20°$ when the northern dipole edge is tilted toward the sun (positive tilt). It should be noted that these elongated magnetic field lines to sustain the raised up narrow plasma sheet are concave. The concave feature may be necessary to maintain a stable magnetotail configuration for a while. In fact, the plasma sheet is stable for 30 minutes and the plasma convection becomes weaker there.

6. Conclusion

We have studied the effect of dipole tilt on the magnetosphere structure and dy-

namics from the two- and three-dimensional MHD simulations as well as a theoretical analysis. An analytical model of the position and shape of the magnetic neutral sheet, which is applicable to all the dipole tilt angles, has been proposed and compared with the MHD simulation results. There was quite good agreement between the simulation result and the analytical model. Moreover, the neutral sheet model is consistent with the empirical neutral sheet model given by Fairfield for small dipole tilt.

The central plasma sheet and the magnetic neutral sheet for $B_x = 0$ are together raised along the magnetic equator in the midnight meridian and become gradually parallel to the solar wind flow direction in the distant tail when the northern edge of the geomagnetic dipole is tilted toward the sun. The neutral sheet has an arched shape and is depressed below the geocentric solar magnetospheric equatorial plane near the flanks. At the same time the plasma sheet with lower plasma pressure also expands toward the southern lobe near the midnight meridian.

The inclusion of the IMF allows the mixture between the plasma in the ring plasma sheet and the hot plasma in the magnetosheath even when the dipole axis points to the sun. This is because the tail magnetic reconnection occurs in the antiparallel field region in which the draped IMF neutralizes the tilted dipole field. Therefore, a very complicated dynamic behavior of the plasma sheet can be expected for a larger tilt angle. A successive simulation study will be necessary to elucidate more clearly the magnetotail dynamics, the polar cap phenomena and the local time dependence of the neutral sheet on the effect of dipole tilt.

Acknowledgments

This work was supported by a Grant-in-Aid for Science Research from the Ministry of Education, Science and Culture, by the NASA Solar Terrestrial Theory Program Grant NAGW-78. The simulations were performed at the Computer Center of the Institute of Plasma Physics, Nagoya University, the Computer Center of Nagoya University, the Computer Center of the Institute of Astronautical Science, and the San Diego Supercomputer Center.

References

Bame, S.J., J.R. Asbridge, H.E. Felthauser, E.W. Hones, and I.B. Strong, Characteristics of the plasma sheet in the earth's magnetotail, *J. Geophys. Res.*, *72*, 113, 1967.

Bowling, S.B., The influence of the direction of the geomagnetic dipole on the position of the neutral sheet, *J. Geophys. Res.*, *76*, 5155, 1974.

Bowling, S.B., and C.T. Russell, The position and shape of the neutral sheet at $30 - R_E$ distance, *J. Geophys. Res.*, *81*, 270, 1976.

Fairfield, D.H., A statistical determination of the shape and position of the geomagnetic neutral sheet, *J. Geophys. Res.*, *85*, 775, 1980.

Fairfield, D.H., and N.F, Ness, Configuration of the geomagnetic tail during substorm, *J. Geophys. Res.*, *75*, 7032, 1970.

Gosling, J.T., D. J. McComas, M.F. Thomsen, S.J. Bame, and C.T. Russell, The warped neutral sheet and plasma sheet in the near-earth geomagnetic tail, *J. Geophys. Res.*, *91*, 7093, 1986.

Murayama, T., Spatial distribution of energetic electrons in the geomagnetic tail, *J. Geophys. Res.*, *71*, 5547, 1966.

Ness, N.F., M.H. Acuna, K.W. Behannon, L.F. Burlaga, J.E.P. Connerney, R.P. Lepping, and F.M. Neubauer, Magnetic fields at Uranus, *Science*, *233*, 85, 1986.

Ogino, T., A three dimensional MHD simulation of the interaction of the solar wind with the earth's magnetosphere: The generation of field-aligned currents, *J. Geophys. Res.*, *91*, 6791, 1986.

Ogino, T., R.J. Walker, M. Ashour-Abdalla, and J.M. Dawson, An MHD simulation of B_y-dependent magnetospheric convection and field-aligned currents during northward IMF, *J. Geophys. Res.*, *90*, 10835, 1985.

Rosenbauer, H., H. Grunwaldt, M.D. Montgomery, G. Paschmann, and N. Sckopke, Heos 2 plasma observations in the distant polar magnetosphere: The plasma mantle, *J. Geophys. Res.*, *80*, 2723, 1975.

Russell, C.T., and K.I. Brody, Some remarks on the position and shape of the neutral sheet, *J. Geophys. Res.*, *72*, 6104, 1967.

Siscoe, G.L., Two magnetic tail models for Uranus, *Planet. Space Sci.*, *19*, 483, 1971.

Speiser, T.W., and N.F. Ness, The neutral sheet in the geomagnetic tail: Its motion, equivalent currents and field line reconnection through it, *J. Geophys. Res.*, *72*, 131, 1967.

Voigt, G.-H., A mathematical magnetospheric field model with independent physical parameters, *Planet. Space Sci.*, *29*, 1, 1981.

Voigt, G.-H., The shape and position of the plasma sheet in earth's magnetotail, *J. Geophys. Res.*, *89*, 2169, 1984.

Voigt, G.-H., T.W. Hill, and A.J. Dessler, the magnetosphere of Uranus: Plasma sources, convection, and field configuration, *Astrophys. J.*, *266*, 390, 1983.

Wu, C.C., The effects of dipole tilt on the structure of the magnetosphere, *J. Geophys. Res.*, *89*, 11048, 1984.